J Mater Sci: Mater Med (2011) 22:2781–2789
DOI 10.1007/s10856-011-4454-9

Chemical stability and antimicrobial activity of plasma sprayed bioactive $Ca_2ZnSi_2O_7$ coating

Kai Li · Jiangming Yu · Youtao Xie · Liping Huang · Xiaojian Ye · Xuebin Zheng

Received: 16 June 2011 / Accepted: 29 September 2011 / Published online: 15 October 2011

Abstract Calcium silicate ceramic coatings have received considerable attention in recent years due to their excellent bioactivity and bonding strength. However, their high dissolution rates limit their practical applications. In this study, zinc incorporated calcium silicate based ceramic $Ca_2ZnSi_2O_7$ coating was prepared on Ti-6Al-4V substrate via plasma spraying technology aiming to achieve higher chemical stability and additional antibacterial activity. Chemical stability of the coating was assessed by monitoring mass loss and ion release of the coating after immersion in the Tris–HCl buffer solution and examining pH value variation of the solution. Results showed that the chemical stability of zinc incorporated coating was improved significantly. Antimicrobial activity of the $Ca_2ZnSi_2O_7$ coating was evaluated, and it was found that the coating exhibited 93% antibacterial ratio against *Staphylococcus aureus*. In addition, in vitro bioactivity and cytocompatibility were confirmed for the $Ca_2ZnSi_2O_7$ coating by simulated body fluid test, MC3T3-E1 cells adhesion investigation and cytotoxicity assay.

Kai Li and Jiangming Yu are contributed equally to this work.

K. Li · Y. Xie · L. Huang · X. Zheng (✉)
Key Laboratory of Inorganic Coating Materials, Shanghai Institute of Ceramics, Chinese Academy of Sciences, 1295 Dingxi Road, Shanghai 200050, People's Republic of China
e-mail: xbzheng@mail.sic.ac.cn

J. Yu · X. Ye
Department of Orthopaedics, Changzheng Hospital, Second Military Medical University, Shanghai 200003, People's Republic of China

1 Introduction

Calcium silicate (Ca–Si) based ceramics, such as $CaSiO_3$ [1, 2] and Ca_2SiO_4 [3], are regarded as potential bioactive materials for skeletal tissue applications [4] owing to their superior bioactivity and biocompatibility. Although the beneficial effects on bone response have been confirmed, clinic usage of Ca–Si based ceramics is still limited due to their poor mechanical property. There are considerable interests in Ca–Si based ceramics as coating materials on metallic substrates in which high mechanical strength and excellent bioactivity can be guaranteed simultaneously. Thermal spraying, especially plasma spraying, is a favorable and commonly used method for biomedical coating deposition [5]. Plasma sprayed $CaSiO_3$ and Ca_2SiO_4 coatings have shown not only better bioactivity but also enhanced bonding strength with titanium alloy as compared with HA coating [6]. However, major drawbacks of the calcium silicate coatings are their high dissolution rate and induction of high pH values in surrounding physiological environment retarding cell growth and thereby affecting their osseointegration ability [4, 7]. Recently, several metal elements such as Ti and Zr incorporated Ca–Si based ceramic coatings have been prepared, and improved chemical stability were achieved for these coatings in physiological environment [8, 9]. Zinc is an important trace element in human bone and has been found to play an important role in bone growth and replication of related DNA [10, 11], which was also used to reinforce bioceramics such as HA [12] and calcium silicates [13].

Infections are common problems when biomaterials are implanted into human body, which are usually caused by adherence and colonization of bacterial on biomaterials. As a biomedical coating, an endowed antibacterial property can prevent bacterial growth on its surface and hence

reduce the risk of biomaterial-associated infections [14]. Zinc is an essential antioxidant and anti-inflammatory agent in human body, deficiency in which usually causes delayed wound healing, immune dysfunction, growth retardation, and neurosensory disorders [10]. The antimicrobial action of Zn^{2+} ion is less extensive than that of Ag^{+}, however, the usage of Zn^{2+} instead of Ag^{+} can also avoid some demerits such as toxicity to host cells and causing severe inflammatory responses [15]. So far, there are few reports regarding the potential use of zinc incorporated Ca–Si based ceramics or coatings as antimicrobial implants.

In the present study, zinc was incorporated into Ca–Si system and thus $Ca_2ZnSi_2O_7$ powder was synthesized, which was used as a feedstock to prepare coating on Ti-6Al-4V substrate via plasma spraying. The aim of the study was to investigate the chemical stability and antimicrobial activity of the $Ca_2ZnSi_2O_7$ coating. In vitro bioactivity, cell adhesion behavior and cytotoxicity of the coating were evaluated as well in this study.

2 Materials and methods

2.1 Sample preparation and characterization

$Ca_2ZnSi_2O_7$ powder was synthesized by the sol–gel method using zinc nitrate hexahydrate ($Zn(NO_3)_2{\cdot}6H_2O$, SCRC, China), calcium nitrate tetrahydrate ($Ca(NO_3)_2{\cdot}4H_2O$, SCRC, China), and tetraethyl orthosilicate [$(C_2H_5O)_4Si$, TEOS, SCRC, China] as raw materials. The detailed preparation procedure has been described by Wu, et al. [16]. The prepared powder was sieved to 80 meshes and then sprayed on Ti-6Al-4V substrates with dimensions of 10 × 10 × 2 mm and φ16× 2 mm, respectively. The coating plates of 10 × 10 × 2 mm were used for chemical stability and bioactivity evaluation, and the disk samples with dimension of φ16 × 2 mm were employed for antibacterial tests and in vitro cell culture experiments. An atmosphere plasma spray (APS) system (F4-MB, Sulzer Metco, Switzerland) was applied to fabricate $Ca_2ZnSi_2O_7$ coating under modified spray parameters listed in Table 1. The thickness of the fabricated coating was around 170 μm. Before plasma spraying, the substrates were ultrasonically cleaned in acetone, and then grit blasted using corundum sand of F60 grade. For comparison, pure $CaSiO_3$ coating was fabricated in the same condition.

Table 1 Plasma spraying parameters

Spray parameters	
Argon plasma gas flow rate (slpm)	40
Hydrogen plasma gas flow rate (slpm)	10
Spray distance (mm)	100
Argon powder carrier gas (slpm)	3.5
Current (A)	650
Voltage (V)	68
Powder feed rate (g/min)	25

Crystalline phases of the obtained $Ca_2ZnSi_2O_7$ powder and coating were analyzed by X-ray diffraction (XRD, D/max 2500 V, Rigiku, Japan), using Cu Kα radiation at 40 kV and 100 mA, while crystallinity of the coating was calculated by MDI Jade 5.0 software. Surface microstructure of the coatings was observed by field emission scanning electron microscopy (FE-SEM, JSM-6700, JEOL, Japan), and surface roughness (Ra) was measured using surface test apparatus (T8000, Hommel werke, Germany).

Bonding strength between the $Ca_2ZnSi_2O_7$ coating and Ti-6Al-4V substrate was assessed according to ASTM C633. In performing the tests, cylindrical Ti-6Al-4V rods (diameter of 25.4 mm and length of 25.4 mm) were used. One rod with coating (about 380 μm thick) was bonded to the other one without coating but sandblasted by using a thin layer of adherence glue (E-7, Shanghai institute of synthetic resin, China) whose tensile fracture strength is over 70 MPa. After drying 3 h at 100°C in an oven at ambient atmosphere, the bonding strength was measured using a mechanical tester (Instron-5592, SATEC, USA) at a crosshead speed of 2 mm/min. The average of five test data was taken as the value of bonding strength.

2.2 Chemical stability and bioactivity evaluations

For evaluating the chemical stability of the $Ca_2ZnSi_2O_7$ coating, specimens were immersed in 50 ml Tris–HCl buffer solution. The buffer solution was prepared by dissolving 50 mM tris-hydroxymethyl-aminomethane [$(CH_2OH)_3CNH_2$] in deionized water and then balanced at pH 7.40 with hydrochloric acid (HCl) at 37°C. After soaking for 1, 4, 7, and 14 days, mass losses of the coating were measured. The changes in pH values of the solution were measured and the Ca, Si, Zn ion concentrations in Tris–HCl buffer solution were determined using inductively coupled plasma atomic emission spectroscopy (ICP-AES, Vista AX, Varian, USA). The pure $CaSiO_3$ coating was used as comparison.

Simulated body fluid (SBF) test was carried out to examine the bioactivity of the $Ca_2ZnSi_2O_7$ coating. After being ultrasonically washed in acetone and rinsed in deionized water, coating specimen was soaked in SBF solution whose ion concentrations nearly equal to those of the human body blood plasma, as shown in Table 2. SEM with electron probe X-ray microanalysis (EPMA, JXA-8100, JEOL, Japan) was used to observe surface morphology and determine element composition of the coating after immersion in SBF at 37°C for 4 weeks.

Table 2 Ion concentration of SBF in comparison with human blood plasma

Concentration (mM)								
	Na^+	K^+	Ca^{2+}	Mg^{2+}	HCO_3^-	Cl^-	HPO_4^{2-}	SO_4^{2-}
SBF	142.0	5.0	2.5	1.5	4.2	147.8	1.0	0.5
Blood plasma	142.0	5.0	2.5	1.5	27.0	103.0	1.0	0.5

2.3 Antibacterial test

Bacteria used were the Cowan I strain of *Staphylococcus aureus*, a common cause of implant-associated infections bacteria. The bacteria were grown overnight in nutrient broth at 37°C, followed by centrifuging. The treated bacteria were then suspended and diluted to 10^6 cells/ml with sterilized water. Four pieces of Ti-6Al-4V disks ($\varphi 16 \times 2$ mm) coated by $Ca_2ZnSi_2O_7$ were placed in sterilized tubes followed by the addition of 20 ml PBS and 0.2 ml of the diluted cell suspension. Four Ti-6Al-4V disks without coating were used as blank control. The tubes were incubated at 37°C with shaking at 150 rpm for 18 h. After finishing the incubation, 0.5 ml of the harvested inoculum in the sterilized tubes was diluted with PBS at volume ratios of 10^{-2} and 10^{-3}, respectively. 0.2 ml of these dilution series were then inoculated onto nutrient agar plates and cultured at 37°C for 48 h. The number of colonies formed on the agar was counted and three plates were assessed to obtain an average value. The antibacterial ratio K was calculated by the following formula:

$$K = (A - B)/A \times 100\%$$

where A is the average number of the bacteria colonization for the control sample, and B is the average number of bacteria colonization for the testing sample.

2.4 In vitro cell culture

MC3T3-E1 cells, a mouse calvaria-derived osteoblast-like cell line (Chinese Academy of Sciences Cell Bank), were cultured at 37°C in a 5% CO_2 incubator in plastic dishes containing α-minimal essential medium (α-MEM, Gibco, USA) supplemented with 10% fetal bovine serum (FBS, Gibco, USA), 100 U/ml of penicillin and 100 mg/ml of streptomycin. They were subcultured every 2–3 days using 0.2% trypsin plus 0.02% EDTA in Ca^{2+}/Mg^{2+}-free phosphate-buffered saline (PBS).

2.5 Morphology of MC3T3-E1 cells on samples

For the sake of investigating earlier cell adhesion behavior on the $Ca_2ZnSi_2O_7$ coating, in vitro cell culture in 24-well plates was carried out and the MC3T3-E1 cells were used. The cells were cultured on the $Ca_2ZnSi_2O_7$ coating surface at an initial concentration of 10^4 cells/cm^2 and incubated for 24 h in α-MEM culture medium supplemented with 10% FBS at 37°C. After 24 h, the disks were removed from the culture wells and rinsed with PBS twice to remove unattached cells and fixed with 2.5% glutaraldehyde solution for 30 min, washed three times (15 min each wash) with 0.1 M PBS. After then, the specimens were dehydrated treating with graded ethanol solutions (50, 70, and 90%) and final dehydration in absolute ethanol twice. The specimens were then observed with scanning electron microscope (SEM, S-4800, Hitachi, Japan). Ti-6Al-4V, a commonly used clinical metallic material, was employed as the counterpart.

2.6 Cytotoxicity test

Cytotoxicity test was carried out according to ISO/EN 10993-5 using extracts of the $Ca_2ZnSi_2O_7$ coating, which was prepared by adding the $Ca_2ZnSi_2O_7$ coating specimen to serum-free α-MEM culture medium at a ratio of 2 cm^2/ml (specimen to medium). After incubation at 37°C for 72 h the supernatant was collected. Serial diluted extracts (1.00, 0.500, 0.250, 0.125, and 0.0625 cm^2/ml) were prepared using serum-free α-MEM. Subsequently, the diluted extracts were sterilized by filtration (0.22 μm). MC3T3-E1 cells at a density of 10^4 cells/cm^2 were seeded into 96-well plates and incubated for 24 h before culture medium was removed and replaced by 50 μl of α-MEM supplemented with 10% FBS and 50 μl of appropriate concentration extracts. The culture medium supplemented with 10% FBS without the addition of diluted extracts was used as a blank control (Blank). A solution of 50 μl of 0.2% Triton X-100 and 50 μl of α-MEM medium supplemented with 10% FBS was used as a negative control (Ctr−). The cells were incubated for 2 days and then their proliferation were evaluated using MTS assay (Promega, Madison, WI, USA) where 10 μl 3-(4,5-dimethylthiazol-2-yl)-2, 5-diphenyltetrazolium bromide (MTS, Huamei Biochem, Shanghai, China) was added to one of the wells and allowed to incubate for 4 h. Measurement of the absorbance was carried out at 490 nm by microplate reader (SPECTRA MAX PLUS 384 MK3, Thermo, USA).

2.7 Statistical analysis

Results were expressed as means ± standard deviation (SD) for all experiments and were analyzed using one-way ANOVA with a post-hoc test. A P-value < 0.05 was considered statistically significant.

3 Results and discussion

3.1 Coating characterization

Phase compositions of the original $Ca_2ZnSi_2O_7$ powder and the as-sprayed coating were shown in Fig. 1, from which it can be seen that XRD patterns of the $Ca_2ZnSi_2O_7$ powder and coating were in agreement with the data in the JCPDS file (Standard Cards No.: 35-0745). The plasma sprayed $Ca_2ZnSi_2O_7$ coating exhibited lower level of crystallinity than the original powder. By using MDI Jade 5.0 software, the crystallinity of the coating was calculated as 67.2%. During plasma spraying process, ceramic powders are heated up to fusion rapidly and re-solidified onto substrates at a high cooling rate of 10^6–10^7 K/s[17], most of the molten particles could not recrystallize in time, and therefore some diffraction peaks broadening with low intensities can be often observed in the XRD patterns of plasma sprayed coatings. Therefore, the crystallinity requirement of the ISO 13779-3 standard for plasma sprayed hydroxyapatite (HA) coatings is only 45%.

Figure 2 shows the surface morphology of the plasma sprayed $Ca_2ZnSi_2O_7$ coating. It can be viewed that the coating had a rough and uneven surface. The surface Ra of the coating was 12.13 ± 0.98 μm. In addition, the bonding strength between the $Ca_2ZnSi_2O_7$ coating and the Ti-6Al-4V substrate obtained in the present study was 33.4 ± 2.2 MPa, which was much higher than the requirement of the international standard for bioactive HA coating implants, i.e., 15 MPa (ISO 13779-2).

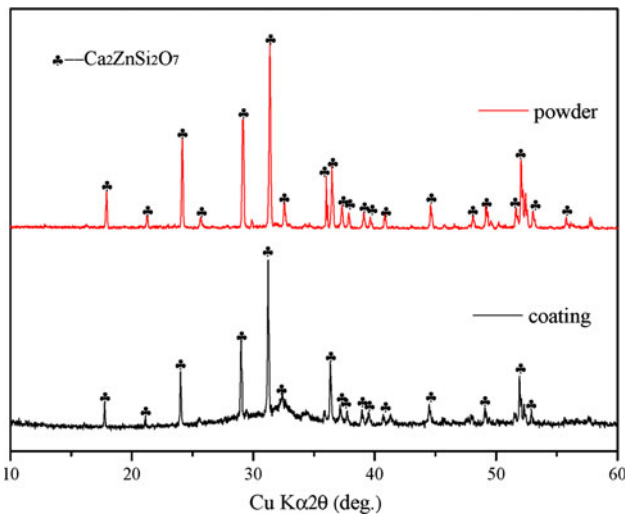

Fig. 1 XRD patterns of the synthesized $Ca_2ZnSi_2O_7$ powder and coating

3.2 Chemical stability and bioactivity

Long-term stability of the coatings is an important factor affecting the performance of implants. Degradability in a biological environment always leads to disintegration of the coatings and usually results in loss of bonding strength and loose of implant fixation. Comparison of mass losses for the $Ca_2ZnSi_2O_7$ and $CaSiO_3$ coatings after immersion in Tris–HCl buffer solution is shown in Fig. 3. It can be seen from Fig. 3 that the mass losses of the $Ca_2ZnSi_2O_7$ coating were much lower compared with those of the $CaSiO_3$ coating. After 14 days immersion in the buffer solution, the mass losses for the zinc-containing Ca–Si based coating was only about one-fifth for the zinc-free

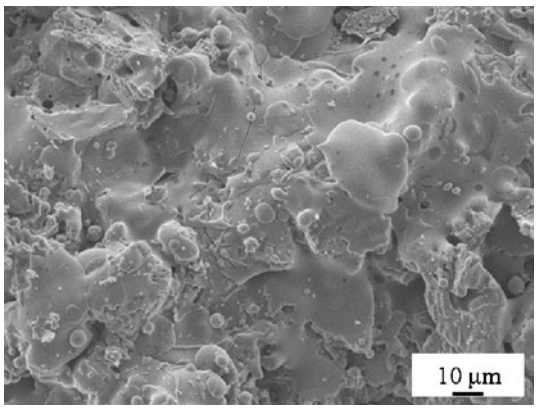

Fig. 2 Surface micrograph of $Ca_2ZnSi_2O_7$ coating

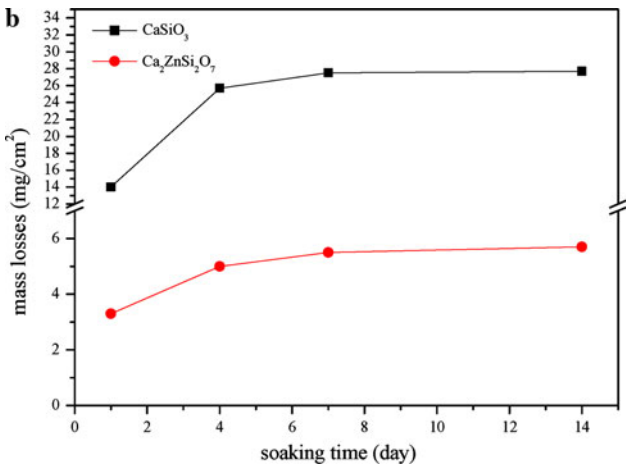

Fig. 3 Mass losses of the coatings immersed in Tris–HCl buffer solution

coating. ICP-AES analysis demonstrated a much reduced Ca and Si ions release of the $Ca_2ZnSi_2O_7$ coating than that of the $CaSiO_3$ coating in Tris–HCl buffer solution, as shown in Fig. 4a, b. Release of Zn ion (Fig. 4c) was also detected for the $Ca_2ZnSi_2O_7$ coating, which could have a positive function in antimicrobial effect of the coating. The pH value variation of Tris–HCl buffer solution after immersion of the coating is given in Fig. 5. The figure reveals that the pH values of the solution increased quickly after the immersion of the $CaSiO_3$ coatings, however, the pH values for the $Ca_2ZnSi_2O_7$ coating were obviously lower and after 14 days it became stable. The appropriate control of pH value in surrounding environment around biomedical implant is one of crucial factors to reduce negative response of bone tissue [18].

Chemical stability of plasma sprayed biomedical coatings is a valuable characteristic affecting long-term stability of the implants. The high dissolution rate of pure calcium silicates limits their applications as coating implants [8]. In this study, plasma sprayed $Ca_2ZnSi_2O_7$ coating exhibited an obviously improved chemical stability as compared with $CaSiO_3$ coating, which might be related to the crystal structure of $Ca_2ZnSi_2O_7$. $Ca_2ZnSi_2O_7$ belongs to sorosilicates, which have two silicate tetrahedrons that are linked by one oxygen ion and thus the basic chemical unit is $[Si_2O_7]^{6-}$. Zn^{2+} is in four coordination and it is speculated that ZnO_4 tetrahedron and Si_2O_7 group can form a more stable network that binds Ca^{2+} ions [19], and then, the stability of $Ca_2ZnSi_2O_7$ coating is improved.

A material which forms apatite in SBF is expected to form apatite in vivo and bond to living bone, that is, show bioactivity [20]. In our study, after 28 days immersion in SBF, apatite formation was observed on the $Ca_2ZnSi_2O_7$ coating as shown in Fig. 6. Under higher magnification, it could be observed that the particles were composed of plenty of worm-like micro-grains, which is one of the typical morphologies of the bone-like apatite formed in vitro [21]. Figure 7 shows the SEM photographs and the EDS spectra scanning along the polished cross-section line of $Ca_2ZnSi_2O_7$ coatings soaked in SBF for 28 days. From

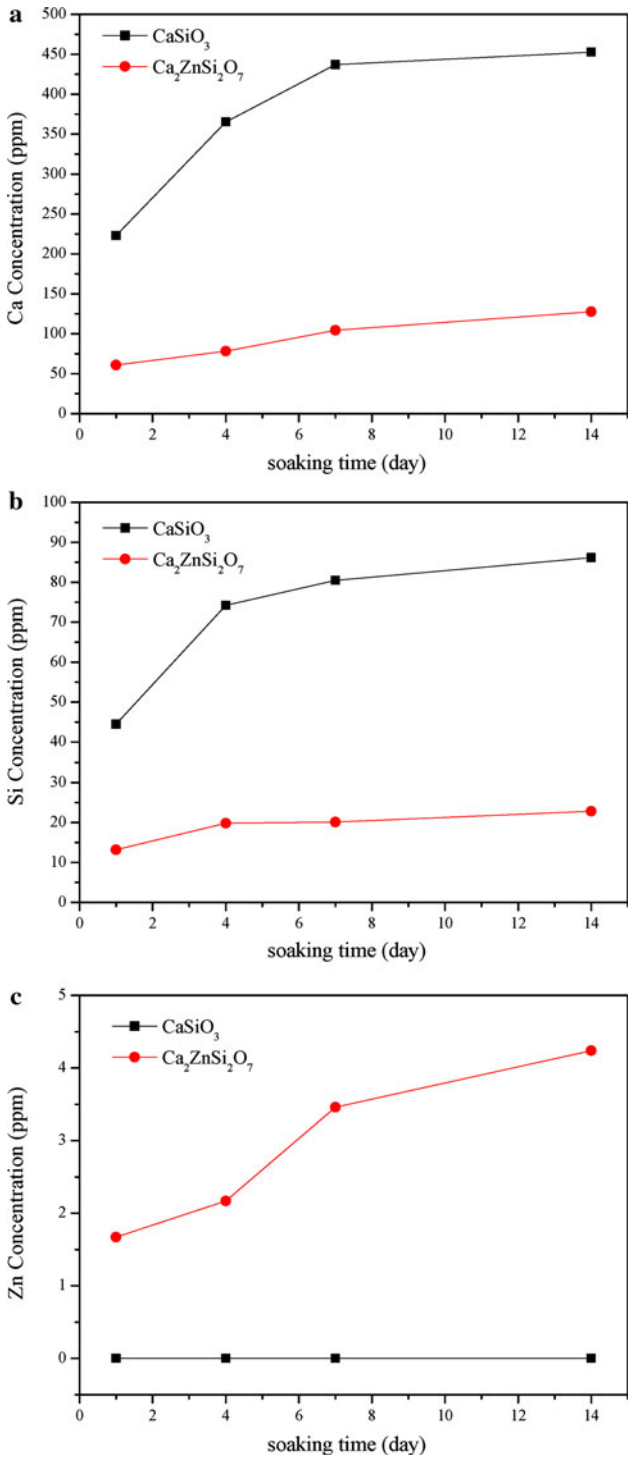

Fig. 4 Ca ions (**a**), Si ions (**b**), and Zn ions (**c**) release of the coatings in Tris–HCl buffer solution

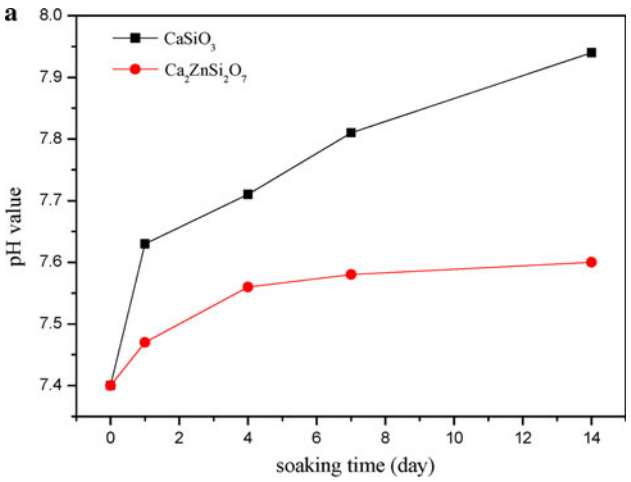

Fig. 5 Changes of pH values for the coatings immersed in Tris–HCl buffer solution

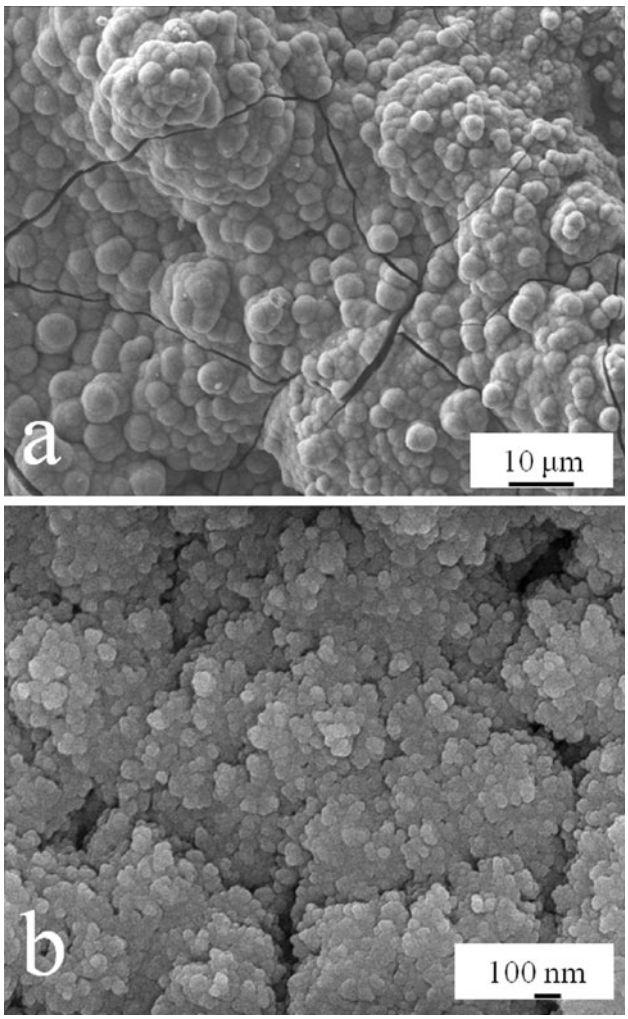

Fig. 6 Surface SEM image of the $Ca_2ZnSi_2O_7$ coating after 28 days immersion in SBF solution (**a**) and its higher magnification (**b**)

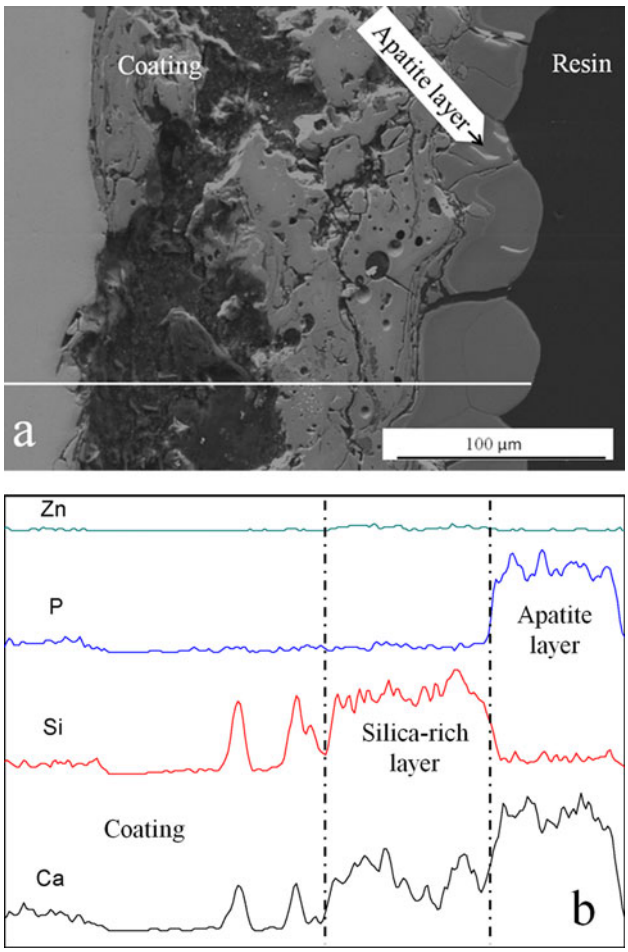

Fig. 7 **a** SEM photograph and **b** EDS spectra scanning along the line on the polished cross-section of $Ca_2ZnSi_2O_7$ coating soaked in SBF solution for 28 days

Fig. 7, two layers having different compositions are observed on the surface of the coating. The top layer was apatite layer which was mainly composed of Ca and P and had a Ca/P molar ratio around 1.6. Under the apatite layer, a silica-rich layer was found, which might result from the ionic exchange between Ca^{2+} in the coating and H^+ within the SBF solution. Chemical stability and apatite formation ability in SBF are usually considered as two paradoxical factors [13], which are normally difficult to be obtained at the same time. In the present study, the incorporation of zinc in the calcium silicate coating did not significantly suppress the apatite formation on the coating, but improved the chemical stability of the coating.

3.3 Antimicrobial activity

As reported by researchers and clinicians, bacterial contamination during implant placement and extensive inflammation of the wound may delay healing of the soft and hard tissues [22]. Biomaterial-associated infections constitute a major clinical problem and often necessitate implant replacement [23]. Based on this reason, it is necessary to establish a biomaterial which offers enough stability and bioactivity, as well as antimicrobial property. Antimicrobial effect of the $Ca_2ZnSi_2O_7$ coating against *S. aureus* is shown in Fig. 8. It can be seen that the number of viable bacteria on the $Ca_2ZnSi_2O_7$ coating decreased sharply as compared with that on the biomedical Ti-6Al-4V substrate (the control). Comparison of total colony forming unit (CFU) between the $Ca_2ZnSi_2O_7$ coating and the Ti-6Al-4V substrate shown in Fig. 9 indicates that the CFU for the coating was much less than that for the control. The calculated antibacterial ratio of the $Ca_2ZnSi_2O_7$ coating against *S. aureus* was high to 93%.

It is obvious that zinc plays a determining role in the antibacterial effect for the coating. However, the mechanism of inhibitory action of zinc on bacteria is only partially known. Several proposals have developed to explain the inhibitory effects of Zn^{2+} ions on bacteria. Gross et al.

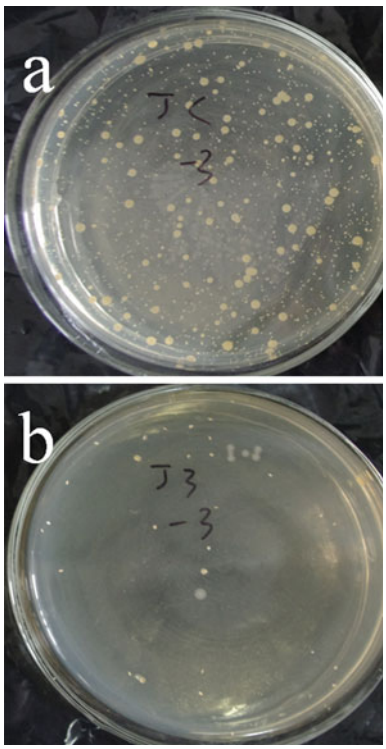

Fig. 8 Representative photos of viable *S. aureus* after 18 h interaction with Ti-6Al-4V (**a**) and $Ca_2ZnSi_2O_7$ coating (**b**)

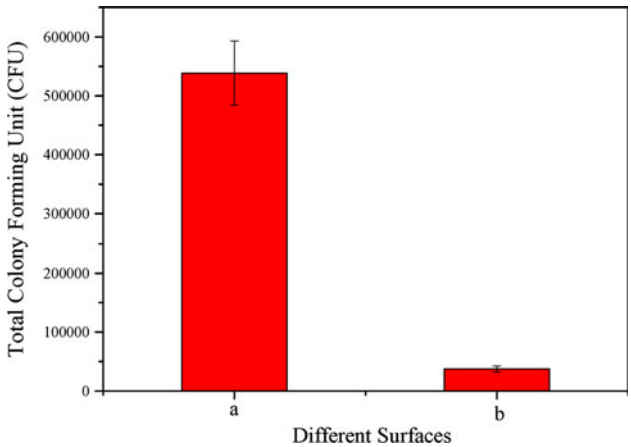

Fig. 9 Total CFU of *S. aureus* after 18 h interaction with Ti-6Al-4V (**a**) and $Ca_2ZnSi_2O_7$ coating (**b**)

[24] demonstrated that teichoic acids on the *S. aureus* cell wall carry a negative charge, which may be favorable for zinc ions attaching onto the bacteria. It was hypothesized that zinc ions eluted from the coating affected the bacterial outer membrane, causing the formation of irregularly shaped pits in the outer member. This structural modification induced changes in membrane permeability, resulting in cell death finally [25]. Some other studies suggested that heavy metals react with protein of the bacteria by combining the SH groups, which leads to the inactivation of the proteins [26–28]. The antimicrobial mechanism of the $Ca_2ZnSi_2O_7$ coating will be investigated in our further study.

3.4 In vitro cytocompatibility

In vitro cytocompatibility of the $Ca_2ZnSi_2O_7$ coating was evaluated by observation of the morphology of MC3T3-E1 cells cultured on the coating surface. Cell adhesion and spreading belong to the first phase of cell-material interactions, and are also probably the most critical stage. The quality of the first phase will influence the cell's capacity for proliferation and differentiation [29]. SEM images of the MC3T3-E1 cells on the $Ca_2ZnSi_2O_7$ coating and Ti-6Al-4V titanium alloy are shown in Fig. 10. It can be seen that after 24 h incubation, cells attached and spread well on the $Ca_2ZnSi_2O_7$ coating surface (Fig. 10a, c). Fine filopodia (red circles in Fig. 10a, c) which facilitate the interaction between cells and coating clearly appeared. Furthermore, confluence and connection among cells were also observed (blue circles in Fig. 10a). In contrast, fewer cells were observed on the control, Ti-6Al-4V substrate (Fig. 10b, d). Generally speaking, the MC3T3-E1 cells on the Ti-6Al-4V showed some signs of spreading but were not comparable to the $Ca_2ZnSi_2O_7$ coating where the cells were well elongated, spread, and appeared more confluent. It could be deduced that the $Ca_2ZnSi_2O_7$ coating can offer a favorable environment for attachment and spread of osteoblast cells.

3.5 Cytotoxicity test

The effect of ions released from $Ca_2ZnSi_2O_7$ coatings on the proliferation of MC3T3-E1 cells was examined and the results are shown in Fig. 11. The results showed that the proliferation of MC3T3-E1 cells increased with decreasing concentrations of extracts from the $Ca_2ZnSi_2O_7$ coatings. Absorbance of extracts with concentrations from 0.125 to 1.00 cm^2/ml showed no significant difference compared to that of the blank control. It showed a slight decrease at higher concentration (2 cm^2/ml) and increase at lower concentration (0.0625 cm^2/ml), compared to the blank control. It can be concluded that the $Ca_2ZnSi_2O_7$ coatings show no toxic effect on the MC3T3-E1 cells.

4 Conclusions

$Ca_2ZnSi_2O_7$ powder synthesized by sol–gel method was deposited onto titanium alloy substrate by plasma spraying. The $Ca_2ZnSi_2O_7$ coating exhibited significantly improved stability in physiological solution, in comparison with $CaSiO_3$ coating, owing to the incorporation of zinc in the

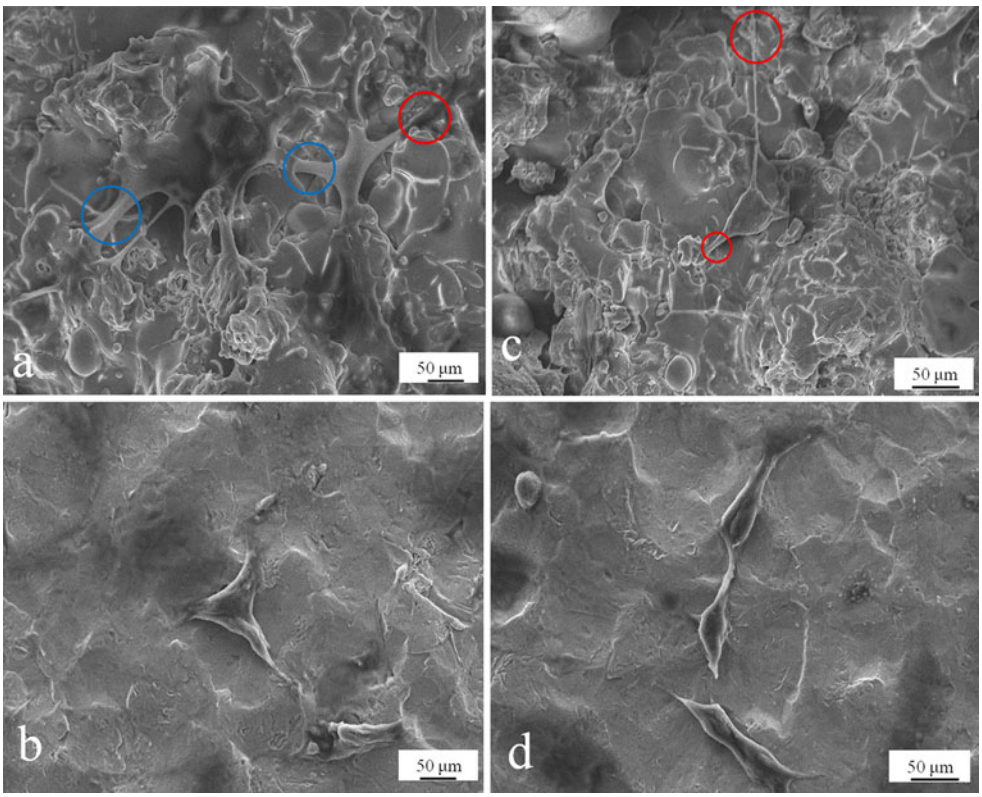

Fig. 10 SEM photographs showing morphology of $Ca_2ZnSi_2O_7$ coating (**a**, **c**) and Ti-6Al-4V (**b**, **d**) cultured with MC3T3-E1 cells for 24 h

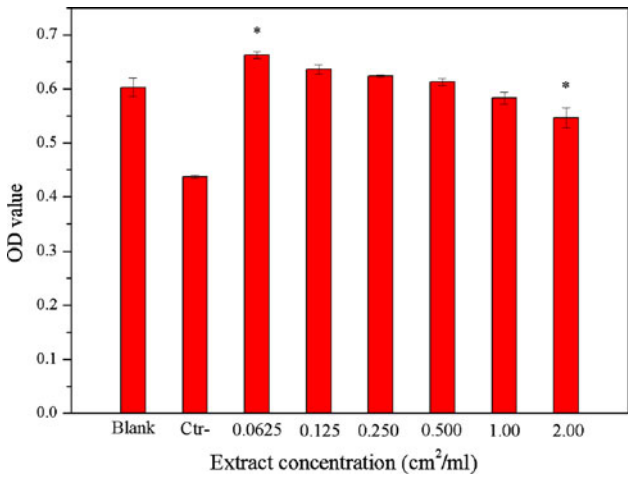

Fig. 11 Cytotoxic evaluation of different concentrations of the $Ca_2ZnSi_2O_7$ coating extracts at 2 days of culture. *The experimental group compared with the blank control group, $P < 0.05$. *Blank*: blank control; *Ctr*−: negative control

calcium silicate coating. Bacterial colonization study exhibited an obviously reduced number of *S. aureus* after interaction with $Ca_2ZnSi_2O_7$ coating, and antibacterial ratio high to 93% was achieved for the coating. The coating exhibited good bioactivity as well as high bonding strength with the titanium alloy substrate. In vitro cell adhesion observation indicated that MC3T3-E1 cells can attach and spread well on the $Ca_2ZnSi_2O_7$ coating surface, and no cytotoxicity was found during the extracts assay of the coating.

Acknowledgments This study was supported by the National Natural Science Foundation of China (Grant No. 81071455) and the Fund for Key Science and Technology Program of Shanghai Science and Technology Committee (Grant No. 09441900106).

References

1. Siriphannon P, Kameshima Y, Yasumori A, Okada K, Hayashi S. Influence of preparation conditions on the microstructure and bioactivity of alpha-CaSiO3 ceramics: formation of hydroxyapatite in simulated body fluid. J Biomed Mater Res. 2000;52(1):30–9.
2. De Aza PN, Luklinska ZB, Martinez A, Anseau MR, Guitian F. Morphological and structural study of pseudowollastonite implants in bone. J Microsc-Oxford. 2000;197:60–7.
3. Gou ZG, Chang J. Synthesis and in vitro bioactivity of dicalcium silicate powders. J Eur Ceram Soc. 2004;24(1):93–9.
4. Xue WC, Liu XY, Zheng XB, Ding CX. In vivo evaluation of plasma-sprayed wollastonite coating. Biomaterials. 2005;26(17):3455–60.
5. Sun LM, Berndt CC, Gross KA, Kucuk A. Material fundamentals and clinical performance of plasma-sprayed hydroxyapatite coatings: a review. J Biomed Mater Res. 2001;58(5):570–92.
6. Liu XY, Tao SY, Ding CX. Bioactivity of plasma sprayed dicalcium silicate coatings. Biomaterials. 2002;23(3):963–8.

7. Wu CT, Ramaswamy Y, Soeparto A, Zreiqat H. Incorporation of titanium into calcium silicate improved their chemical stability and biological properties. J Biomed Mater Res A. 2008;86A(2):402–10.
8. Liang Y, Xie YT, Ji H, Huang LP, Zheng XB. Excellent stability of plasma-sprayed bioactive Ca3ZrSi2O9 ceramic coating on Ti-6Al-4V. Appl Surf Sci. 2010;256(14):4677–81.
9. Liu XY, Ding CX. Plasma sprayed wollastonite/TiO2 composite coatings on titanium alloys. Biomaterials. 2002;23(20):4065–77.
10. Tapiero H, Tew KD. Trace elements in human physiology and pathology: zinc and metallothioneins. Biomed Pharmacother. 2003;57(9):399–411.
11. Ma ZJ, Yamaguchi M. Stimulatory effect of zinc on deoxyribonucleic acid synthesis in bone growth of newborn rats: enhancement with zinc and insulin-like growth factor-I. Calcified Tissue Int. 2001;69(3):158–63.
12. Storrie H, Stupp SI. Cellular response to zinc-containing organoapatite: an in vitro study of proliferation, alkaline phosphatase activity and biomineralization. Biomaterials. 2005;26(27):5492–9.
13. Wu CT, Ramaswamy Y, Chang J, Woods J, Chen YQ, Zreiqat H. The Effect of Zn contents on phase composition, chemical stability and cellular bioactivity in Zn–Ca–Si system ceramics. J Biomed Mater Res B. 2008;87B(2):346–53.
14. Chen YK, Zheng XB, Xie YT, Ji H, Ding CX. Antibacterial properties of vacuum plasma sprayed titanium coatings after chemical treatment. Surf Coat Tech. 2009;204(5):685–90.
15. Masse A, Bruno A, Bosetti M, Biasibetti A, Cannas M, Gallinaro P. Prevention of pin track infection in external fixation with silver coated pins: clinical and microbiological results. J Biomed Mater Res. 2000;53(5):600–4.
16. Wu CT, Chang J, Zhai WY. A novel hardystonite bioceramic: preparation and characteristics. Ceram Int. 2005;31(1):27–31.
17. Gell M, Jordan EH, Sohn YH, Goberman D, Shaw L, Xiao TD. Development and implementation of plasma sprayed nanostructured ceramic coatings. Surf Coat Tech. 2001;146:48–54.
18. Wu CT, Ramaswamy Y, Kwik D, Zreiqat H. The effect of strontium incorporation into $CaSiO_3$ ceramics on their physical and biological properties. Biomaterials. 2007;28(21):3171–81.
19. Zreiqat H, Ramaswamy Y, Wu C, Paschalidis A, Lu Z, James B, et al. The incorporation of strontium and zinc into a calcium–silicon ceramic for bone tissue engineering. Biomaterials. 2010;31(12):3175–84.
20. Kokubo T, Takadama H. How useful is SBF in predicting in vivo bone bioactivity? Biomaterials. 2006;27(15):2907–15.
21. Liu XY, Ding CX. Morphology of apatite formed on surface of wollastonite coating soaked in simulate body fluid. Mater Lett. 2002;57(3):652–5.
22. Esposito M, Hirsch JM, Lekholm U, Thomsen P. Biological factors contributing to failures of osseointegrated oral implants. (II). Etiopathogenesis. Eur J Oral Sci. 1998;106(3):721–64.
23. Campoccia D, Montanaro L, Arciola CR. The significance of infection related to orthopedic devices and issues of antibiotic resistance. Biomaterials. 2006;27(11):2331–9.
24. Gross M, Cramton SE, Gotz F, Peschel A. Key role of teichoic acid net charge in *Staphylococcus aureus* colonization of artificial surfaces. Infect Immun. 2001;69(5):3423–6.
25. Amro NA, Kotra LP, Wadu-Mesthrige K, Bulychev A, Mobashery S, Liu GY. High-resolution atomic force microscopy studies of the *Escherichia coli* outer membrane: structural basis for permeability. Langmuir. 2000;16(6):2789–96.
26. Feng QL, Wu J, Chen GQ, Cui FZ, Kim TN, Kim JO. A mechanistic study of the antibacterial effect of silver ions on *Escherichia coli* and *Staphylococcus aureus*. J Biomed Mater Res. 2000;52(4):662–8.
27. Xua JA, Ding G, Li JL, Yang SH, Fang BS, Sun HC, et al. Zinc-ion implanted and deposited titanium surfaces reduce adhesion of *Streptococccus* mutans. Appl Surf Sci. 2010;256(24):7540–4.
28. Sondi I, Salopek-Sondi B. Silver nanoparticles as antimicrobial agent: a case study on *E. coli* as a model for Gram-negative bacteria. J Colloid Interf Sci. 2004;275(1):177–82.
29. Anselme K. Osteoblast adhesion on biomaterials. Biomaterials. 2000;21(7):667–81.